Facies analysis and diagenetic evolution of the Dinantian carbonates in the Dutch subsurface: data and analyses wells HEU-01 and HEU-01-S1

Report by SCAN

October 2019

Ministerie van Economische Zaken en Klimaat
ebn
TNO
Interreg North-West Europe DGE-ROLLOUT

Facies analysis and diagenetic evolution of the Dinantian carbonates in the Dutch subsurface: data and analyses wells HEU-01 and HEU-01-S1

Written by:
Mahtab Mozafari[1], Peter Gutteridge[2], Alberto Riva[3], Kees Geel[4], Joanna Garland[2] and Julie Dewit[2]

October 2019

1- Energie Beheer Nederland (EBN), Daalsesingel 1, 3511 SV Utrecht, the Netherlands
2- Cambridge Carbonates Ltd, No. 4 The Courtyard, 707 Warwick Road, Solihull, B91 3DA, UK
3- G.E.Plan Consulting srl, Via L. Ariosto 58, 44121 Ferrara, Italy
4- Geological Survey of the Netherlands (TNO), Princetonlaan 6, 3584 CB Utrecht, the Netherlands

Dit rapport is een product van het SCAN-programma en wordt mogelijk gemaakt door het Ministerie van Economische Zaken en Klimaat

Table of contents

4. Heugem-01 (HEU-01 and HEU-01-S1)

4.1 Introduction

The HEU-01 well is located in the southern Maastricht area, SE Netherlands (Figures 4-1 and 4-2, Table 4-1). A subsequent sidetrack was drilled until 502.7 m.

Figure 4-1: Map showing all the wells penetrating the Dinantian carbonates. Location of the HEU-01 well is indicated by dashed red circle.

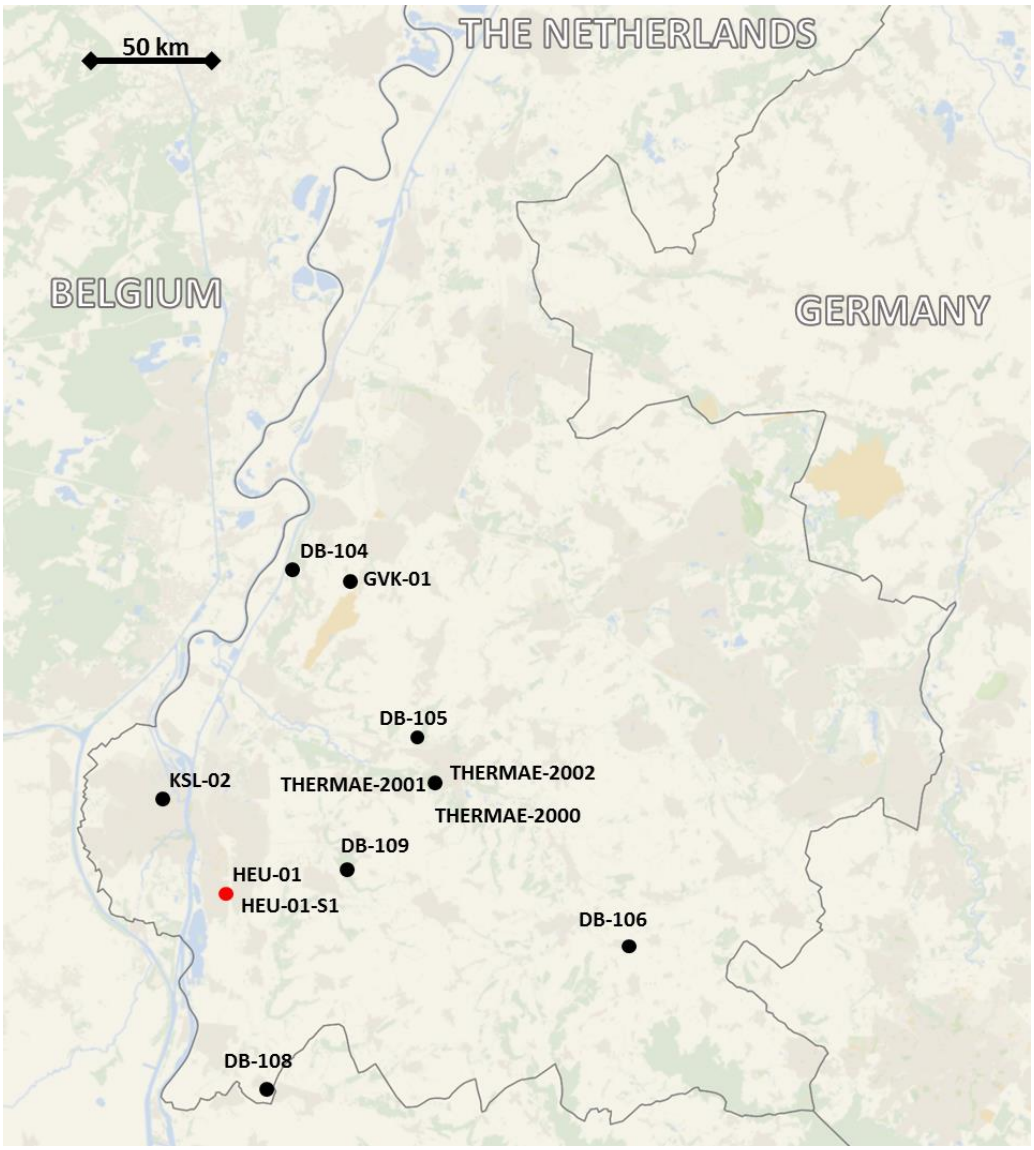

Figure 4-2: Map showing location of the HEU-01 and HEU-01-S1 wells (red circle).

Table 4-1: Coordinates and depth of HEU-01 well (from www.nlog.nl).

Co-ordinates (x, y in utm31, ed50 format)	691150, 5634271
Lat/Long (°)	50.82751857, 5.71413431
Supplied co-ordinates	177950, 315255 (RD)
Depth in meters referred to:	Ground Level
Total depth (m, along hole):	365.1 main hole, 502.7 sidetrack S1
Vertical position of Ground Level:	47.4 meter relative to NAP
Trajectory shape:	Vertical
Deviation in X-direction:	0
Deviation in Y-direction:	0
True vertical depth (TVD) in m:	365.1

Heugem-01 reached to depth of 365.70 m. It has been tried to core the complete Carboniferous interval. This was not possible because of the nature of the silicified, partly brecciated and fractured rocks. Therefore, some 81 m between 114 and 365 m have been drilled with a roller bit. A capacity test yielded some 12 m³ water per hour (piezometric head about 10 m above the surface). It has been tried to re-open the hole with the roller bit, using a very heavy mud fluid. However, at 309.50 m it appeared that instead a new hole was drilled: Heugem-01a. Below 309.50 m, drilling faced many technical problems. Between 309.50 and 402.20 m the string was broken twice. At 402.20 m the string was stuck completely (95 m of string were finally left below in the hole). Coring was continued with a smaller diameter. Between 403 and 502.70 m the fluid loss varied between 20 and 100%. A capacity test for the interval 402.20 and 102.70 m yielded some 24 m³ water per hour (piezometric head about 10 m above the surface).

Table 4-2: Drilling data about HEU-01 well (from www.nlog.nl).

Client name	Gemeente Maastricht
Start date	Apr 1, 1981
End date	Jul 1, 1981
Drilling company	Gruner
Type of well	Water Exploration
Result	Mineral water
Status	Closed-in

4.2 Available dataset

Some documents, including scanned well logs are present on "www.nlog.nl" within the following link:
https://www.nlog.nl/nlog/requestData/nlogp/allBor/metaData.jsp?tableName=BorLocation&id=106519251

The most relevant publications/reports are as follows:

Bless, M. J. M., Boonen, P., Bouckaert, J., Brauckmann, C., Conil, R., Dusar, M., felder, P. J., Felder, W. M., Gökdag, H., Kockel, F., Laloux, M., Langguth, H. R., Van der Meer Mohr, C. G., Meessen, J. P. M. TH., Op het Veld, F., Paproth, E., Pietzner, H., Plum, J., Poty, E., Scherp, A., Schulz, R., Streel, M., Thorez, J., Van Rooijen, P., Vanguestaine, M., Vieslet, J. L., Wiersma, D. J., Winkler Prins, C. F., and Wolf, M. (1981). Preliminary report on Lower Tertiary-Upper Cretaceous and Dinantian-Famennian rocks in the boreholes Heugem-1/1a and Kastanjelaan-2 (Maastricht, the Netherlands). Medelingen Rijks Geologische Dienst, 35, 333-415.

Bless, M. J. M., Bouckaert, J., and Paproth, E. (1981). Vise-Puth: stimulant for further exploration. Annales de La Société Géologique de Belgique, 104, 291-296.

Bless, M. J. M., Bouckaert, J., and Paproth, E. (1983). Recent exploration in pre-Permian rocks around the Brabant Massif in Belgium, the Netherlands and the Federal Republic of Germany. Geologie En Mijnbouw, 62, 51-62.

Bless, M. J. M., Bouckaert, J., Bouzet, P., Conil, R., Cornet, P., Fairon-Demaret, M., Groessens, E., Longerstaey, P., Meesen, J. P. M. T., Paproth, E., Pirlet, H., Streel, M., Amerom, H. W. J. and Wolf, M. (1976). Dinantian rocks in the subsurface north of the Brabant and

Ardenno- Rhenish massifs in Belgium, the Netherlands and the Federal Republic of Germany. Mededelingen Rijks Geologische Dienst, nieuwe serie, 27, 81-195.

Friedrich, G., Bless, M. J. M., Vogtmann, J., and Wiechowski, A. (1987). Lead-zinc mineralization in Dinantian rocks of boreholes Thermae 2000 and Thermae 2002 (Valkenburg A/D Geul, The Netherlands). Annales de La Societe Geologique de Belgique, 110, 59-75.

Laenen, B. (2003). Lithostratigrafie van het pre-Tertiair in Vlaanderen. Deel II: Dinantiaan and Devoon. Vito Report.

Poty, E. (1991). Tectonique de blocs dans le prolongement oriental du Massif du Brabant. Annales de La Société Géologique de Belgique, 114, 265-275. Retrieved from http://popups.ulg.ac.be/0037-9395/index.php?id=1479

Poty, E., and Delculée, S. (2011). Interaction between eustacy and block-faulting in the Carboniferous of the Visé – Maastricht area (Belgium, The Netherlands). Zeitschrift Der Deutschen Gesellschaft Für Geowissenschaften, 162, 117-126. https://doi.org/10.1127/1860-1804/2011/0162-0117

TNO. (1999). Toelichting bij Kaartblad XV Silfard-Maastricht. Geologische Atlas van de Diepe Ondergrond van Nederland.

Van Tongeren, P. C. H. (2006). De Vlaamse Voerstreek: een geologische analyse van het Laat Paleozoïcum van deze regio en van het direct aangrenzend gebied (Vol. 2005/MAT/R).

4.2.1 Logs

The available logs were available as hard copy and were digitised within the frame of SCAN project. The Dinantian section has been extensively logged only in HEU-01-S1. The available log suite is not allowing any formation evaluation, due to missing/non-acquired logs in the middle-upper part of Dinantian successions. The composite gamma ray log of the HEU-01-S1 well is presented in Figure 4-3.

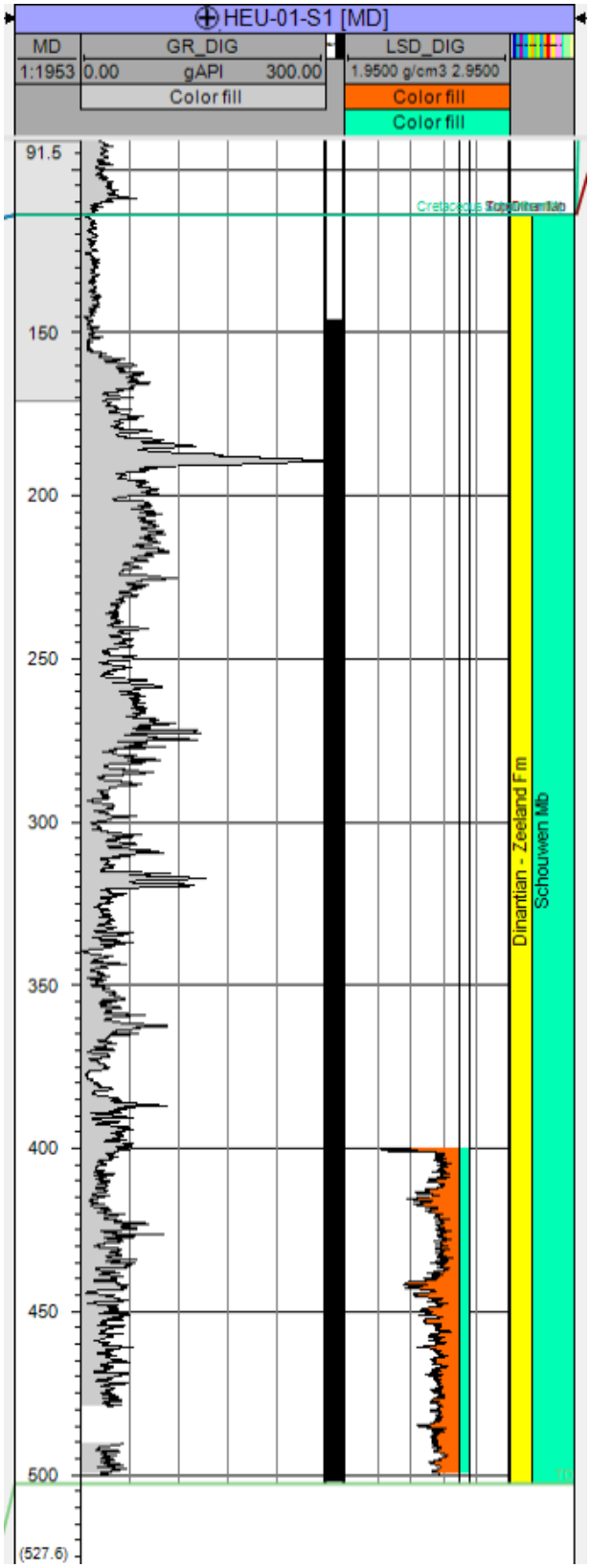

Figure 4-3: Composite gamma ray log of the HEU-01-S1 well, with the indication of the cored section (black bar).

4.2.2 Cores, sidewall cores and cuttings

HEU-01 was cored from 128 to 364 m with several gaps due to drilling problems. HEU-01-S1 was cored in the interval 309.50 to 501 m.

4.2.3 Thin sections

A total number of 68 and 34 thin sections were available for HEU-01 and HEU-01-S1, respectively. All thin sections are from the Schouwen Member. They were studied for their facies and diagenesis within the frame of the SCAN project.

4.2.4 Additional analyses

The following analyses were available (pre-existed) for the HEU-01 well and its sidetrack:

- Chemical analyses with calcimetry (13 samples). A detailed report on elemental concentrations is presented by Bless et al. (1981)
- XRD (14 samples)
- Total and Organic carbon (43 samples)
- Conventional core analyses on plugs (62 samples)
- Vitrinite reflectance (13 samples)

Table 4-3: XRD data (from Bless et al., 1981).

Depth (m)	Sample	Description
132.50-133.70	(LU)	Quartz, kaolinite
132.50-133.70	(LU)	Quartz
133.70-134.00	(LU)	Quartz
134.80	(LU)	Quartz, kaolinite
177.00	(GLA 18151)	Quartz, kaolinite, illite-sericite
216.30	(LU)	Quartz, pyrite, mica, kaolinite
220.00	(GLA 18087)	Quartz, pyrite, illite, kaolinite fireclay, illite-sericite
227.20	(GLA 18088)	Quartz, pyrite, illite, kaolinite fireclay, crandallite
231.40-232.00	(GLA 18155)	Quartz, kaolinite-fireclay, sericite, illite, pyrite, feldspar
264.60-266.70	(GLA 18156)	Quartz, kaolinite fireclay, illite, pyrite- apatite
266.70-268.00	(GLA 18169)	Quartz, pyrite, dolomite, illite, kaolinite-fireclay, apatite
268.90-270.50	(GLA 18157)	Quartz, illite, pyrite, apatite, kaolinite-fireclay
346.50	(LU)	Quartz, calcite, pyrite, mica
360.75	(GLA 18158)	Calcite, quartz, sericite-illite, pyrite

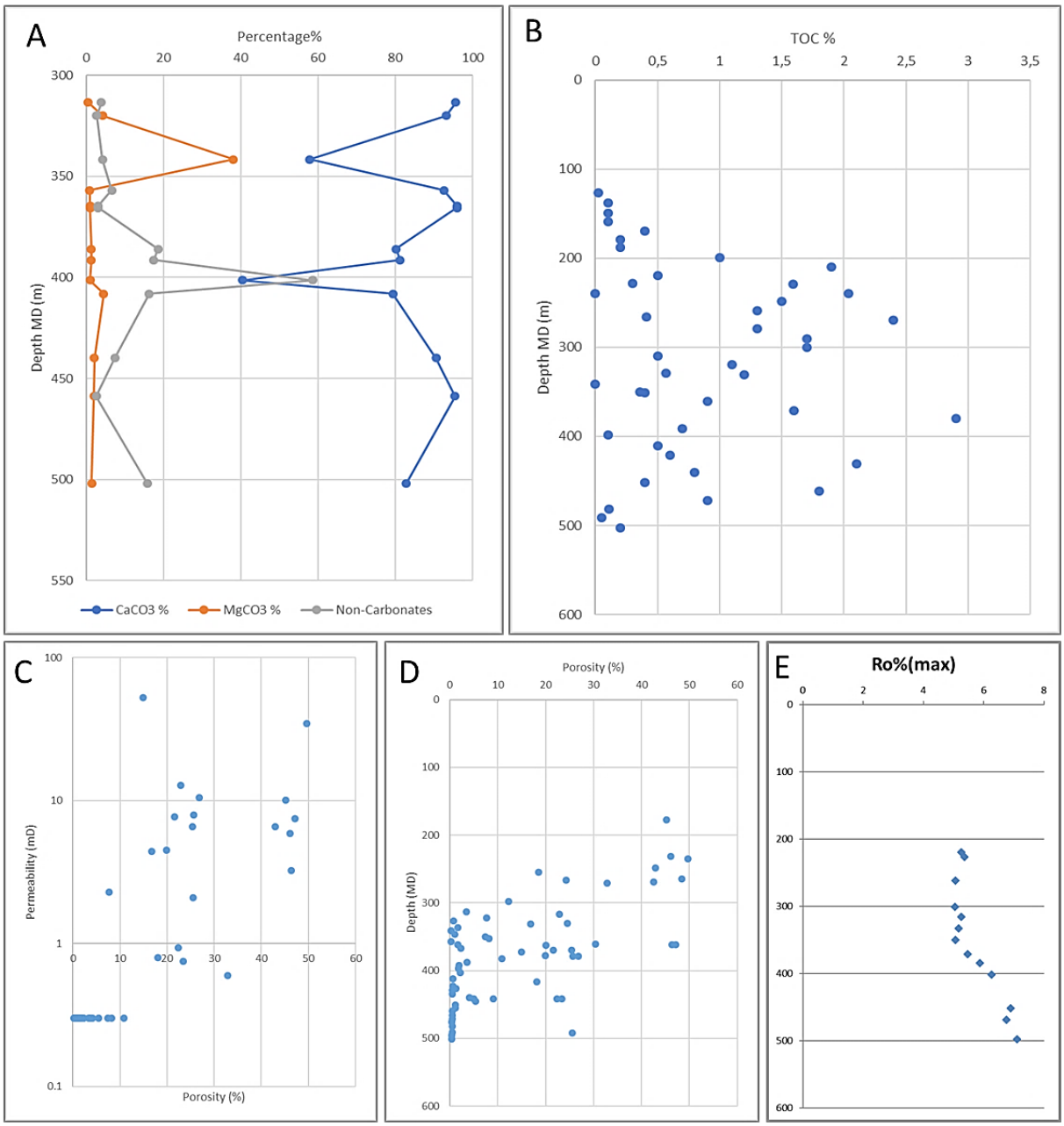

Figure 4-4: Analyses performed by Bless et al. (1981). A) Chemical analyses on the HEU-01 and HEU-01-S1 well samples. B) Total Organic Carbon content in HEU-01 and HEU-01-S01. C, D) Petrophysical analyses for the well HEU-01 and its sidetrack. E) Vitrinite reflectance data in the HEU-01 well and its sidetrack.

4.3 Stratigraphy and sedimentology

The official stratigraphy presented on www.nlog.nl shows that the top of the Dinantian (Schouwen Member) is overlain by the Cretaceous, with the Namurian intervals completely missing. The detailed lithological descriptions of HEU-01 and HEU-01-S1 wells (Table 4-5 and 4-6) are presented in Bless et al. (1981).

Table 4-4: Stratigraphy of the HEU-01 well (from www.nlog.nl).

Stratigraphical Unit	Top Interval	Base Interval
QUATER. UNDIFF.	0	10
Gulpen Fm.	10	82
Vaals Fm.	82	114
Schouwen Mb.	114	502

4.3.1 Dinantian interval

The top of the Dinantian succession is at 114 m, but the coring starts deeper in the section. The upper part of the core is quite unusual and appears completely white, due to strong processes of kaolinisation and silification until 170.40 m (Figure 4-5). In this interval it is possible to observe some thin layers containing framboidal pyrite crystals with a maximum size of 0.5 mm. In the lower part of the interval, some white shales with reddish intercalations which are occasionally brecciated can be observed. Moreover, between 170.40 and 182.30 m, some alternations of white silicified limestones intercalated with back silicified shales is encountered.

Table 4-5: Description of the lithology observed in the HEU-01 well (from Bless et al., 1981).

Depth (m)	Description
114.20	Top Carboniferous
125-148.50	White, silicified shales and carbonates, apparently chalky
148.50-165.00	No data
165-170.40	White, silicified shales and carbonates, apparently chalky, which are occasionally red-coloured in the lower part, locally brecciated.
170.4-174.5	Black shaly silicified ?limestones
174.5-178	White chalky silicified interval
178-180.35	Black silicified shale
180.35-182.30	White chalky silicified interval
182.30-185.70	Silicified interval with black shales and ?limestones
185.70-212.50	No data
212.50-213.50	Silicified interval with black shales and ?limestones
213.50-216	No data
216-274.10	Silicified interval with black shales and ?limestones
301-301.40	Grey, tight bioclastic limestones
309.90-345.00	Grey, bioclastic limestones with slumping structures. In lower part karst dissolution and brecciation
345.00-365.00	(T.D.): Grey to dark-grey, finely stratified, carbonaceous limestone.

Table 4-6: Description of the lithology observed in the HEU-01-S1 well (from Bless et al., 1981).

Depth (m)	Description
310.00-346.00	Grey limestone with slumping structures. In lower part karst dissolution and brecciation.
346.00-368.00	Grey to dark-grey, finely stratified limestone. Occasionally thin laminae and small nodules with presumed pseudomorphs after anhydrite. At 356 m small pseudomorphs after gypsum?
368.00-383.00	Karst dissolution and brecciation. Remnants of laminated limestone.
383.00-394.00	Grey to dark-grey, finely stratified to laminated limestone. At 391 m thin lamina of calcite pseudomorphs after anhydrite.
394.00-402.00	Grey to dark-grey, bioclastic limestone with slumping structures. At 397 m sedimentary breccia with some anhydrite.
402.00-471.00	Grey to dark-grey, finely stratified limestone with thin laminae and small nodules with presumed calcite pseudomorphs after anhydrite. At 431.20 m enterolitic anhydrite with tepee texture in 3 cm thick lens. Between 415 and 479 m slumping structures and karst dissolution. Below 467.50 m development of diagenetic calcareous nodules.
415.00-502.70	(T.D.) Grey to dark-grey, nodular limestone with diagenetic calcareous nodules and load casts. Rare thin laminae and small nodules with calcite pseudomorphs after gypsum

Figure 4-5: Left: 166-177 m, kaolinisation of the core (whitish colour) at the top of dark grey siliceous alteration of basinal Dinantian mudstone. Right: 223-236 m, dark grey siliceous alteration of basinal Dinantian mudstone with white patches of kaolinisation.

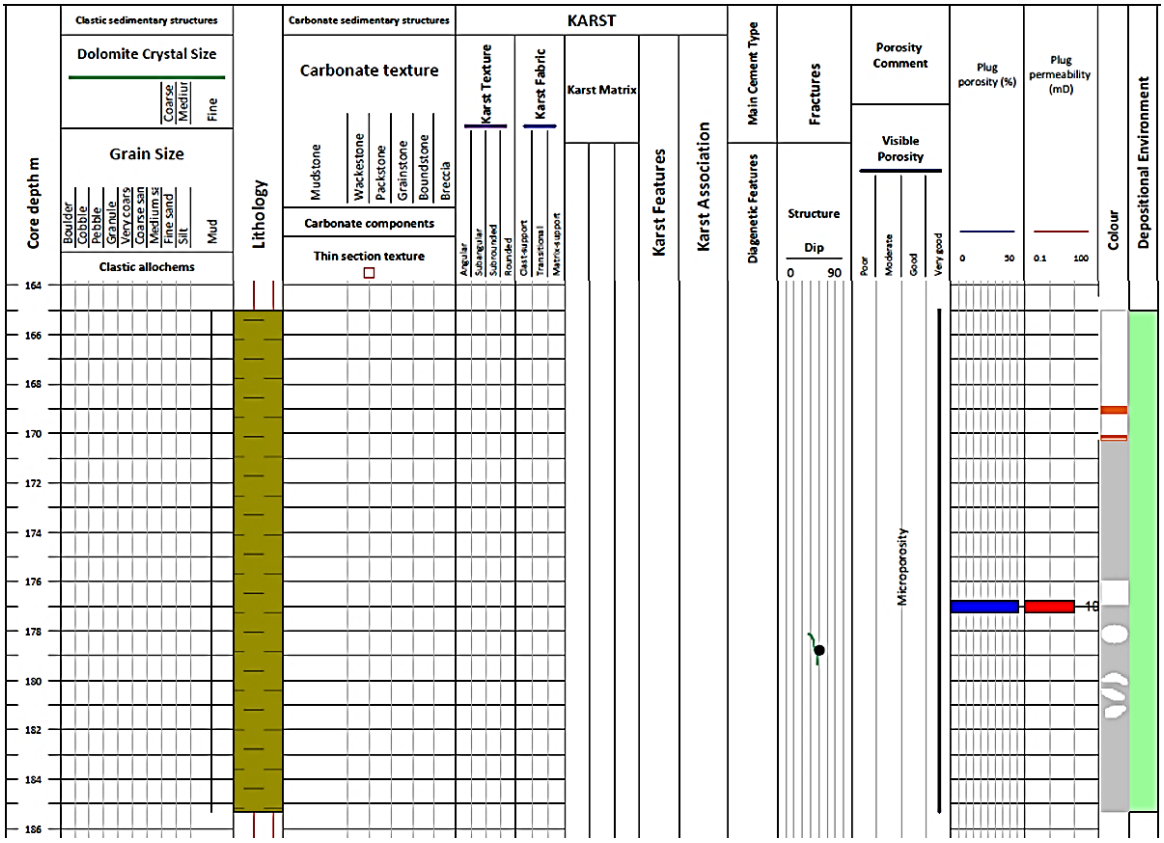

Figure 4-6: Core log interpreted as sub-Cretaceous weathering of the Dinantian basinal facies (constructed in SCAN project).

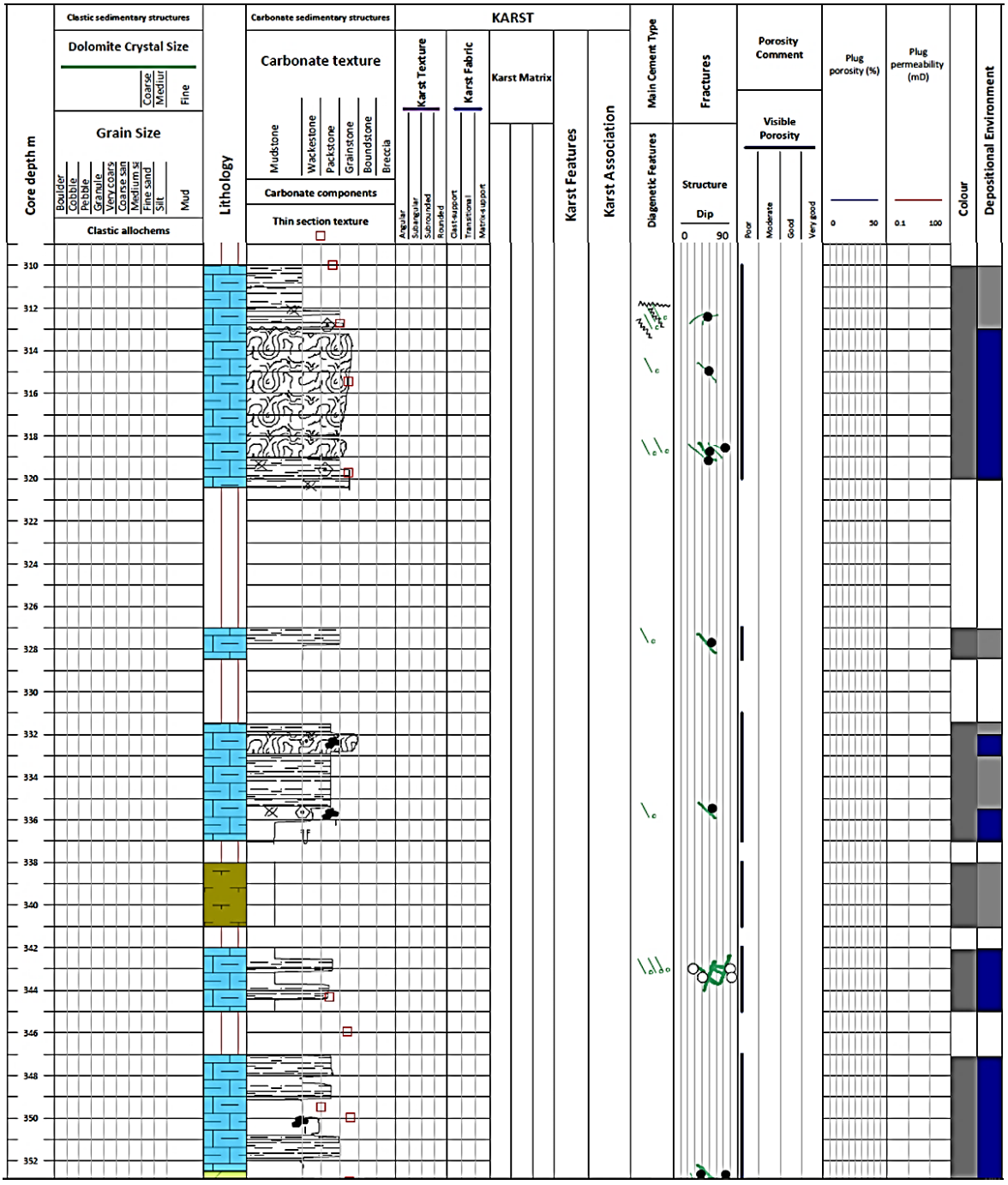

Figure 4-7: Core log of unaltered Dinantian basinal facies at base of Heugem-01 well (constructed in SCAN project).

4.4 Biostratigraphy

Within the frame of the SCAN project, a critical revision of the biostratigraphic attribution presented by Bless et al. (1981) has been performed on the HEU-01 and HEU-01-S1 wells (Table 4-7).

Interval (m)	Original description of Bless et al. (1981)	Observations	Revised Age attribution
114-254	The sequence is poorly known because of the bad preservation of the silicified fossils. This sequence appears to contain elements characteristic of the Cf4 foraminifer zone (V1a-V2a) such as Glomodiscus, as well as forms which might indicate the Cf5 foraminifer zone (V2b-V3a), such as Palaeotextularia and Archaediscus stage concavus and angulatus. Tentatively, this interval is here attributed to the V2a/V2b.	o *Siphonodendron ondulosum* (319.6-321.7 m) appears in the Upper Moliniacian, marking the base of RC5 coral biozone. o *Solenodendron hibernicum* (407.7-407.3 m) is usually appearing in the Lower Visean of Ireland (RC4), while the genus appears around RC3β. o The presence of Archaediscus concavus-angulatus at 120-121 m points to a Cf5 (Livian). o Eostaffella is not diagnostic, as ranges from Visean to Moscovian (183.60-502.7 m)	The upper part has very scarce data. At 120-121 m, the age is probably Livian (Holkerian) – Cf5
309 - 502.70	Numerous forms characteristic of the V2a have been observed (a.o. Koninckopora with double w all, Girvanella densa, Laxoseptabrunsiima, Eotextularia diversa, Pseudolituotubella, Archaediscus (Glomodiscus), Archaediscus stage involutus, Ammarchaediscus (Rectodiscus), Bessiella, Florennella, Eoendothyranopsis, Endospiroplectammina, Dainella, Loeblichia, Planoendothyra and EoparastaffeIla). The absence of Koninckopora with double wall in the basal 13 m should not be taken as an argument for a V1b age. The foraminifers and algae strongly resemble those of the V2a in the Belgian Campine (notably the Halen borehole). The assemblage shows also some resemblance to the V1b deposits of the St.-Ghislain borehole in SW Belgium (Groessens, Henenbert & Conil 1981). Rugose corals are rare in Heugem-1/1a. Only two species have been recognised. *Siphonodendron ondulosum* Poty 1981 in the 319.6-321.7 m sample of Heugem-1 suggests a V2a age (Poty 1981). *Solenodendron hibernicum* (Clarke 1966) has been observed in the 407.7-407.3 m sample of Heugem 1a. This species is only known thus far from Ireland, where it occurs at the boundary of the S2-Dl zones V3a-V3b). However, this is a rare form that may have a much longer stratigraphic range as shown by the present find.	o Girvanella densa (313.00-502.70 m) is Visean, often associated with a V1/V2a assemblage o Laxoseptabrunsiima (313-412 m, cf until 473) is V1-V2a o Eotextularia diversa (344-388 m) is Tn3 to V2a o Pseudolituotubella (365-367 m) is reality only a cf. genus: usually is Cf4 (V1a-V2a) o Archaediscus stage involutus (228.7- 365 m) is usually V2a o Archaediscus (Glomodiscus) (228-502.7 m) is usually considered RC4, with the FAD in MFZ10 (RC4β2) – V1b/V2a. o Ammarchaediscus (Rectodiscus) (312.9-502.70 m) is indicative of CF4 again. o Bessiella (351- 492.30 m – one cf at 183.60-184.4 m) together with Dainella (315-488 m) are typical in the assemblages of RC4 biozone, starting from MFZ8 and passing MFZ11. o Eoendothyranopsis (222.7-412.00 m) covers RC4 and RC5 biozones o Endospiroplectammina (315-502.70 m) is late Tournaisian to Visean o Florennella (345.90-483.25 m - ?183.6) is MFZ9 to MFZ11 (RC4β2 to RC5α) o Loeblichia (358.5- 467 m) is indicating a generic Visean age o Planoendothyra (341-402.15 m) is a generic Tournaisian-Visean microfossil o EoparastaffeIla (355-502.70 m) is Upper Tournaisian (Cf4a1) -Visean (Cf4a2) – MFZ8 to 9, sometimes up to MFZ11	The interval between 121 and 222.70 is uncertain and could be Livian (Holkerian) or late Molinacian (Arundian) Late Molinacian (Arundian) (222.70-321.7 m) Early-mid Molinacian (Arundian-Chadian) – Cf4, from MFZ10 onwards (321-7-502.7 m)

Table 4-7: The biostratigraphic attribution of Bless et al. (1981) and its revision (SCAN project).

4.5 Sequence stratigraphy

Within the framework of the SCAN project, seven depositional cycles have been recognised in the Dinantian succession of HEU-01 that have been grouped as follows according to the gamma-ray character (Table 4-7). The overall depositional setting of the HEU-01 well is interpreted as basinal in which the carbonate intervals was introduced in the form of redeposited platform sediment. The depositional cycles are interpreted in terms of the evolution of surrounding carbonate platforms.

1c and 1d depositional cycles: These depositional cycles are cored in HEU-01 and consist of dolomitised bioclastic wackestone and carbonate mudstone deposited as a distal carbonate ramp facies; the initial low gamma-ray signature reflects the deposition of redeposited carbonates sourced from shallow to mid-ramp settings during the TST. The higher gamma-ray interval represents the drowning of the source of redeposited carbonates during the maximum flooding. The high at the top of the cycle is interpreted as increased supply of redeposited carbonates as the carbonate ramp progrades during the HST. The 1d depositional cycle is cored in HEU-01 and consists of deep water argillaceous limestone and shale.

2a to 2c depositional cycles: These depositional cycles have a higher, more uniform gamma signature, with scattered peaks, they are interpreted as distal ramp or carbonate slope facies, possibly associated with a transition from carbonate ramp- to flat-topped carbonate platform. The low gamma-ray intervals interpreted as influx of resedimented carbonates during high stands. The overall high gamma-ray signature HEU-01 suggests the deposition in a distal basinal setting.

2d to 3a depositional cycles: These depositional cycles show an increasing-upward gamma-ray signature that are interpreted as distal carbonate slope or basinal facies. The high gamma intervals are interpreted LST to TST intervals when there was no carbonate production on platforms on exposed carbonate platforms and no export of peri-platform carbonates to the surrounding basin. The low gamma-ray interval in 3a is interpreted as the effect of the weathering profile combined to the presence of carbonate turbidites, now mostly silicified.

Table 4-8: Sequence stratigraphic scheme used on HEU-01 well.

Depositional cycles	Gamma-ray character	Depositional setting
3b	Gamma ray increases upwards to very high followed by low gamma-ray HST	Condensed deposition in basin during LST and TST; high stand shedding of carbonates into basin.
3a		
2d	Generally high gamma ray.	Distal carbonate ramp or basin.
2c		
2b		
2a		
1d	Moderate to low with moderate to high peaks interpreted as max. flooding followed by low gamma-ray HST	Distal carbonate ramp with increasing carbonate input as ramp progrades during in HST. Max. flooding events marked by high gamma intervals.
1c		

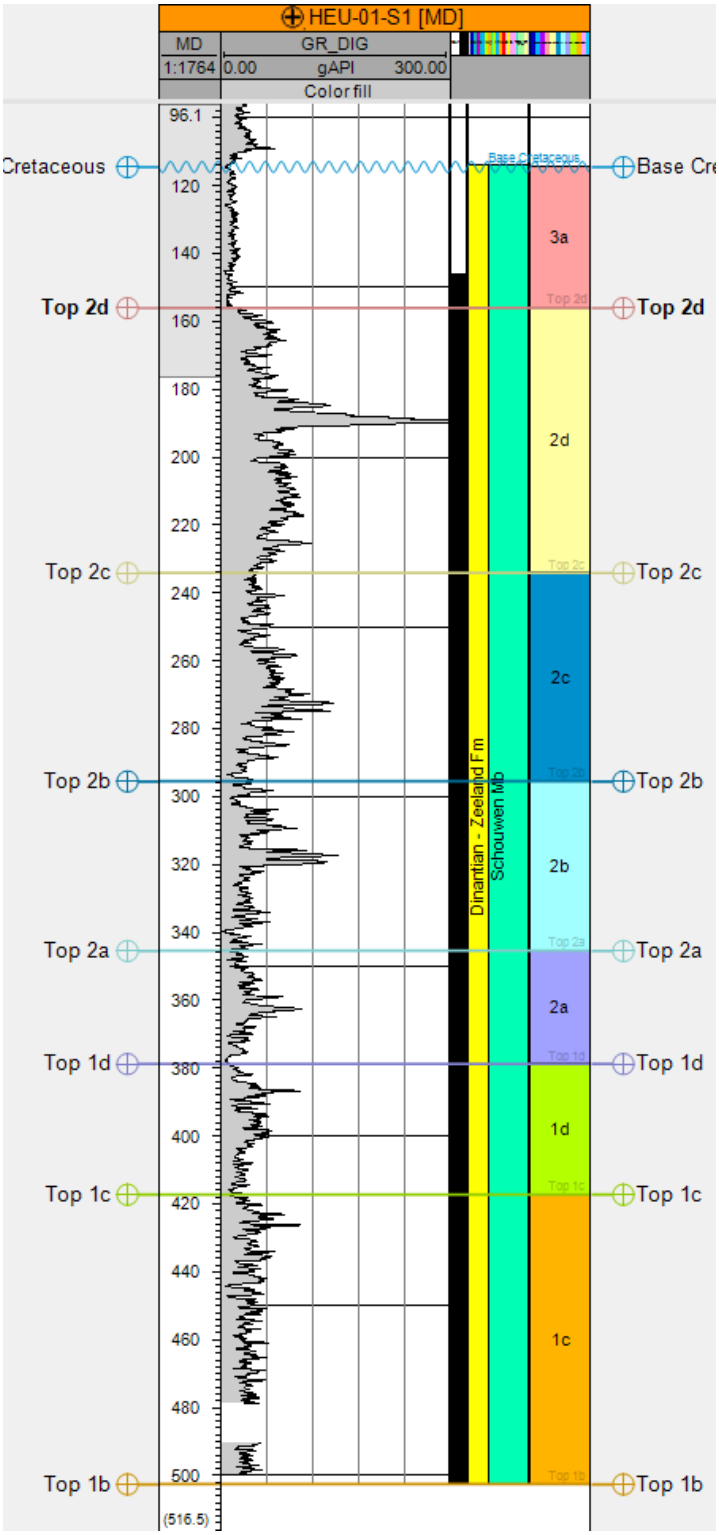

Figure 4-8: Depositional cycles of the HEU-01 well.

4.6 Microfacies

The majority of the limestone textures of the Schouwen Member in the studied thin sections are bioclastic packstones and wackestones, some mudstones occur as well. The Schouwen Member in the HEU-01-S1 are interpreted as resedimented and basinal carbonates (Figures 4-9 and 4-10).

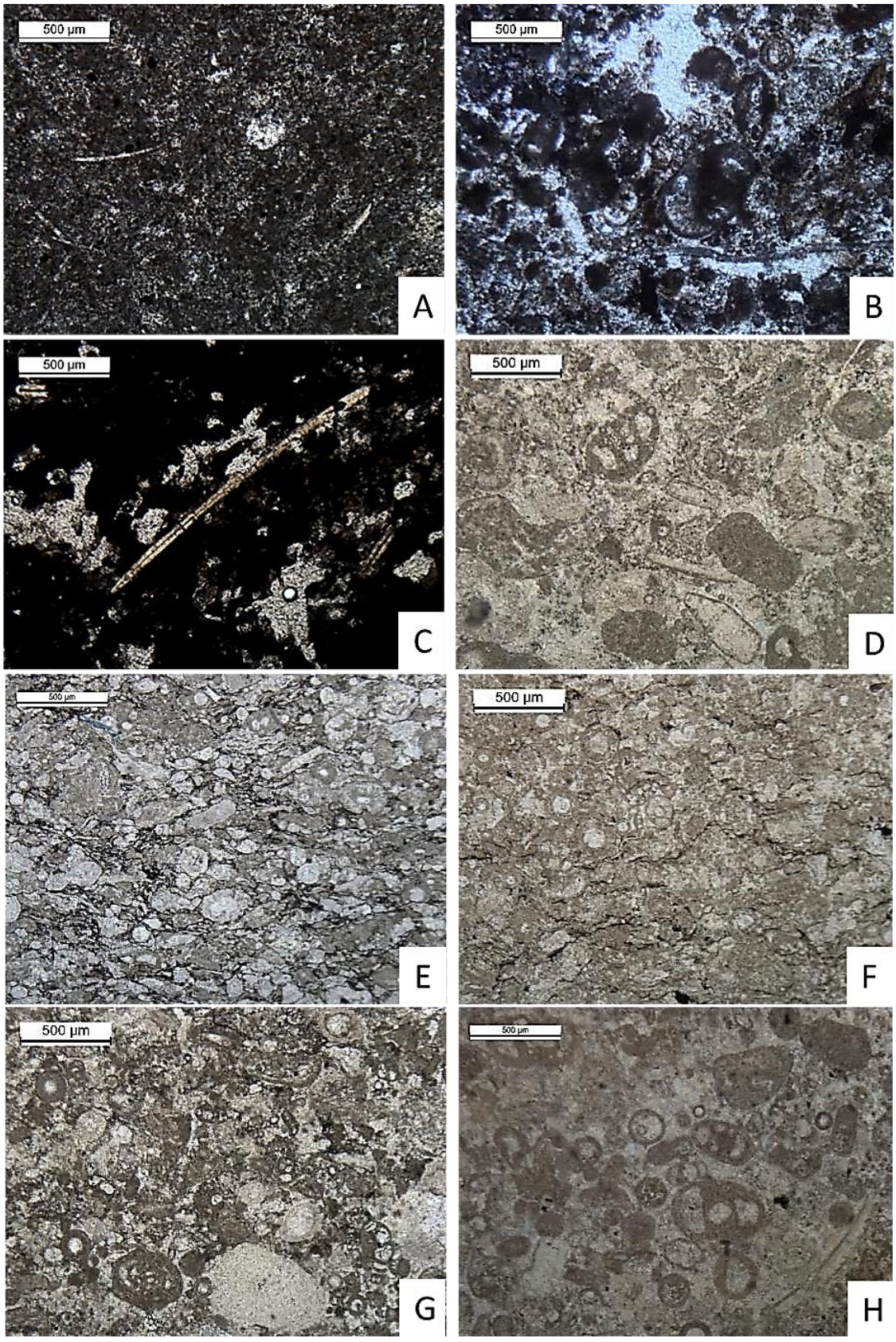

Figure 4-9: A, B) 177 m, argillacoeus peloid packstone. C) 270 m, mudstone with sponges. D) 315.90 m, peloid-bioclastic grainstone. E) 344.50 m, bioclastic packstone. F) 345.90 m, bioclastic grainstone. G) 355 m, bioclastic grainstone. H) 358.50 m, bioclastic grainstone.

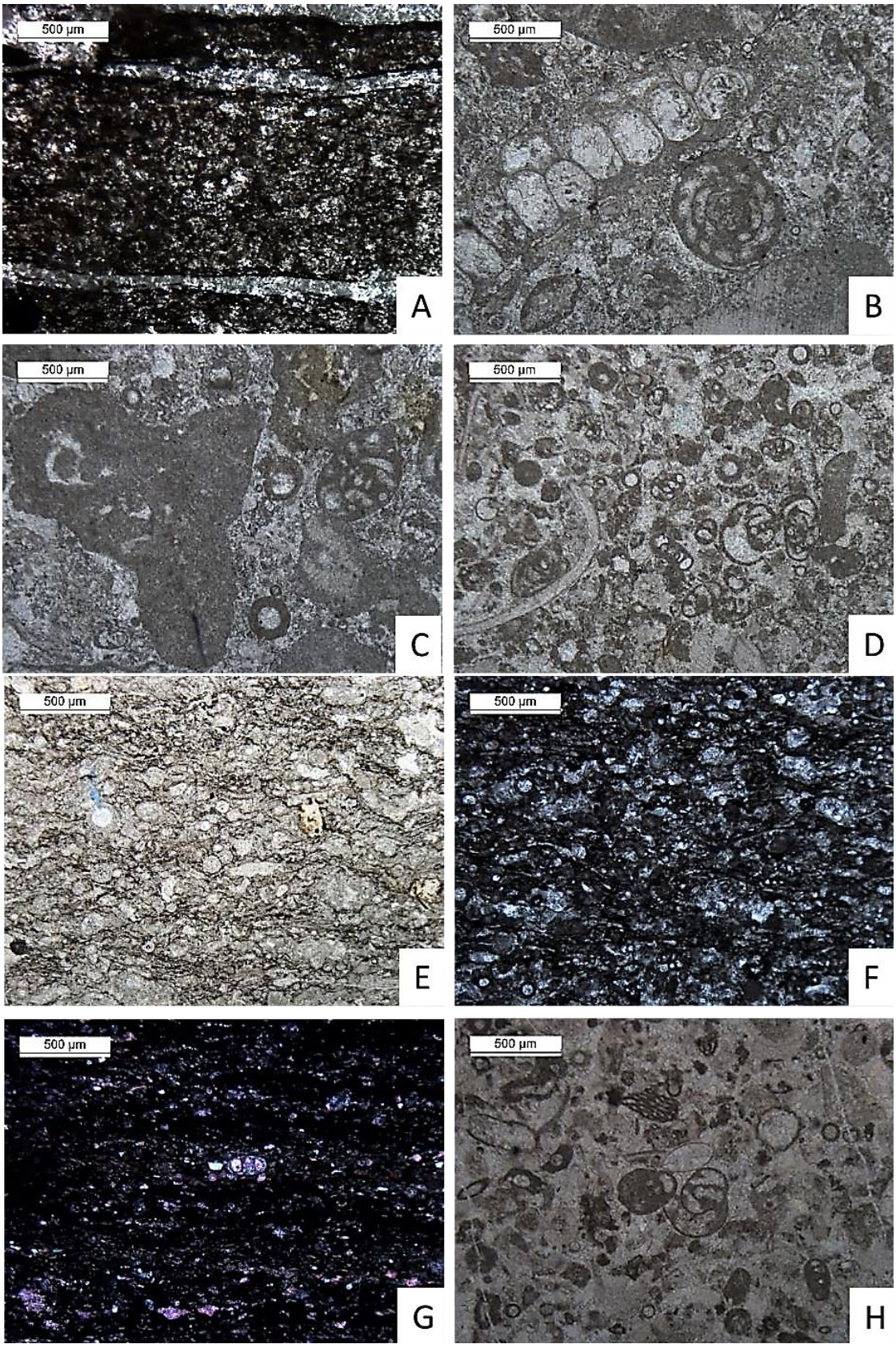

Figure 4-10: A) 367.30 m, laminated pelloidal packstone/mottled mudstone. B) 395.30 m, bioclastic pack-grainstone. C) 395.30 m, bioclastic-intraclastic pack-grainstone. D) 402.15 m, bioclastic grainstone. E) 435.60 m, bioclastic packstone. F) 461.40 m, bioclastic packstone. G) 477.10 m, bioclastic mud-wackestone. H) 502.15 m, bioclastic grainstone.

4.7 Diagenesis

4.7.1 Petrographic observations and paragenetic sequence

A paragenetic sequence was established for the HEU-01-S1 based on the study of existing thin sections (n=102) of the TNO collection. The thin sections are from the Schouwen Member of the Zeeland Formation. The identified paragenetic sequence that has been identified is:

1. Early calcite cements: C1 (+ syntaxial calcite, dissolution of aragonitic components)
2. Early dolomite cement: D1 (volumetrically minor)
3. Equant calcite cement: C2
4. Chemical compaction – stylolites
5. Saddle dolomite + fine crystalline dolomite along stylolites
6. Calcite cemented veins: C3 (no cross cutting relation of the C3 cement and the saddle dolomites is observed in HEU-01 samples. In the KSL-02 samples, calcite veins most likely corresponding to C3 are cross cutting the saddle dolomite. This is why the C3 calcite veins are also interpreted to post-date the saddle dolomites in HEU-01.
7. Silicification: partial or pervasive. Post-dates dolomitisation, post-dates C3. Rarely associated with secondary porosity. Generally non-crystalline quartz, i.e. chert, rare single quartz crystals
8. Recrystallisation: relative timing unknown, see facies for examples.

The paragenetic sequence of diagenetic phases observed in HEU-01-S1 and KSL-02 correspond well (Figure 4-11). Compared to KSL-02, not many samples consist of post-compaction dolomite. It should be noted that in KSL-02 most of the dolomite occurs in the Beveland Member. This unit is not cored in the HEU-01 and HEU-01-S1 wells, instead the younger Schouwen Member is penetrated.

There is no additional data available for further interpretation of the diagenetic processes affecting the Schouwen Member in HEU-01-S1. For further details about the diagenesis of the Dinantian carbonates of the SE Netherlands see KSL-02 report. Photomicrographs showing the main diagenetic phases in the HEU-01-S1 well are presented in Figures 4-12 to 4-15.

HEU-01	KSL-02	GVK	Diagenetic phase
+	+	A?	C1
+	-	MD?	D1
+	+	B?	C2
+	+	+	Stylolites
+	+	-	D2
+	+	-	C3
+	+	+	Si
+	+	-	Recrystallisation

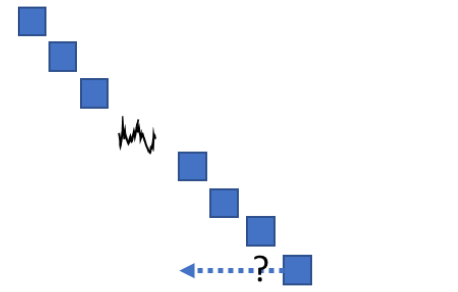

Figure 4-11: Overview of the diagenetic phases and their presence in the HEU-01-S1, KSL-02 and GVK-01.

4.7.2 Diagenetic sequence in the context of burial/thermal history

The diagenetic evolution of this well is very similar to KSL-02. Section 7 (KSL-02) presents detailed information on burial and thermal history of these two wells.

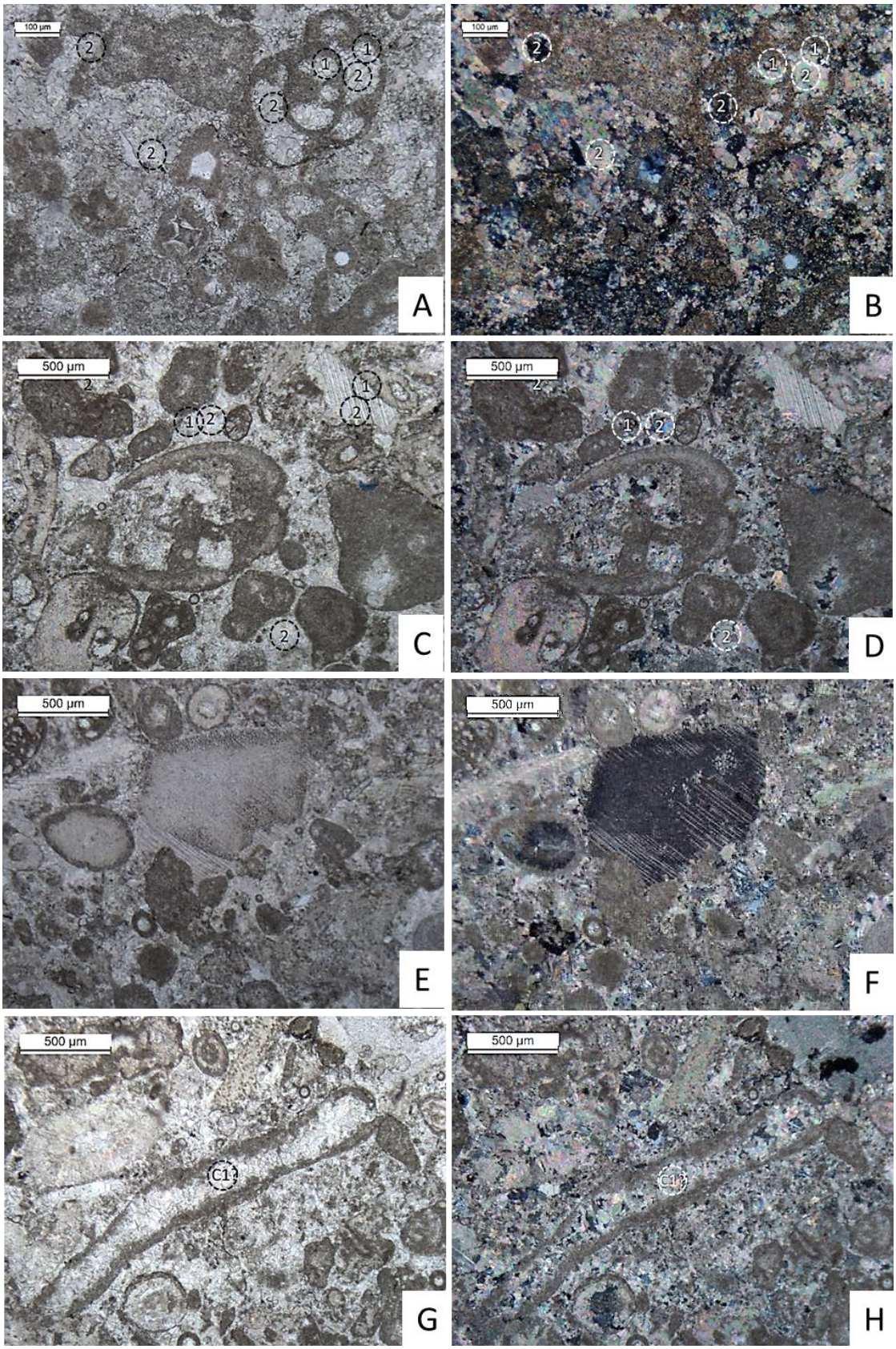

Figure 4-12: Photomicrographs showing the PPL and corresponding XPL images of calcite cements in HEU-01-S1, 407.80 m. A, B) C1 - fine crystalline calcite fringing components, C2 - equant calcite cementing pore space. C, D) C1 - fine crystalline calcite fringing components, C2 - equant calcite cementing pore space. E, F) Syntaxial calcite. G, H) Aragonitic components replaced by C1?.

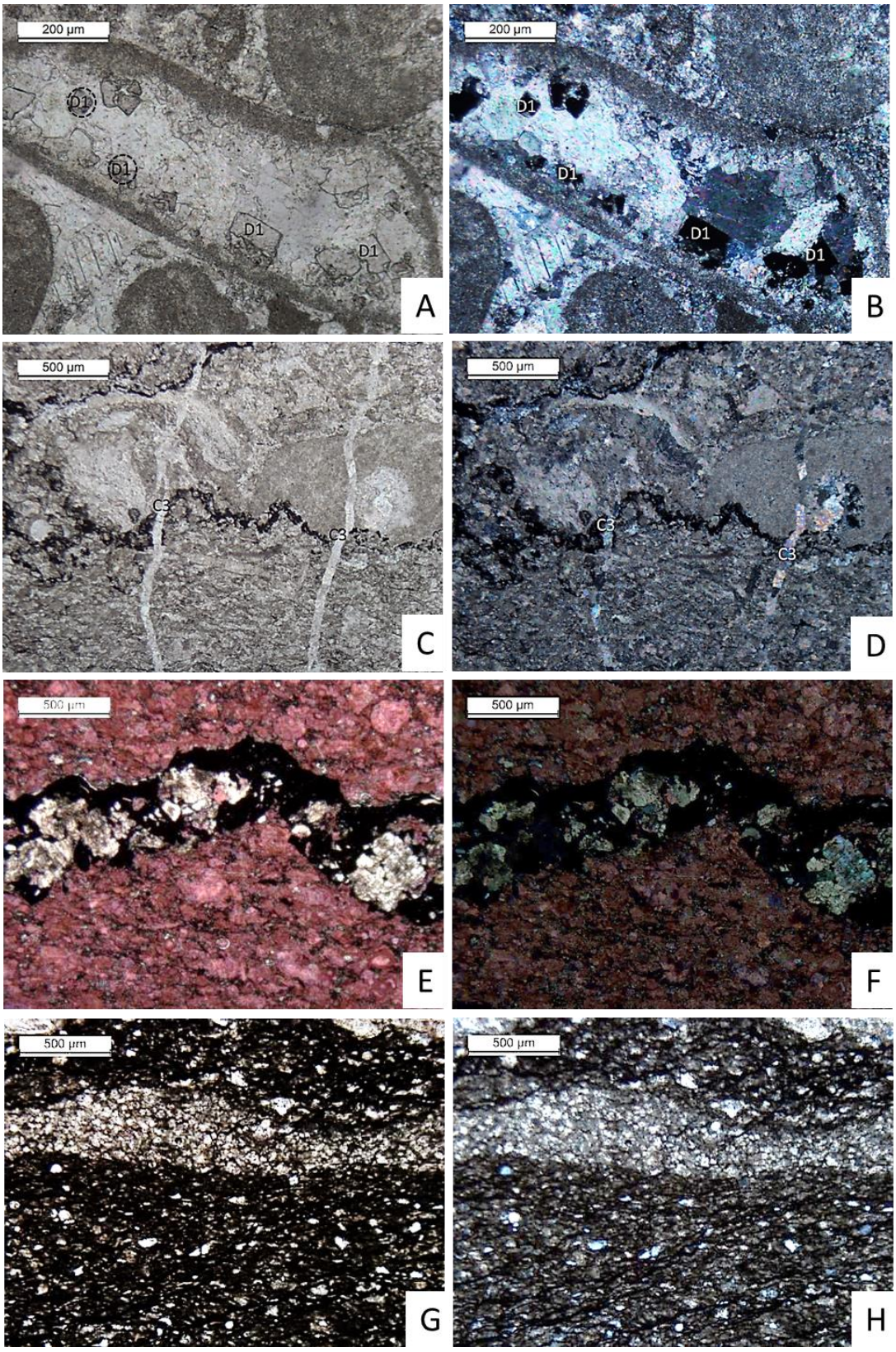

Figure 4-13: Photomicrographs showing the PPL and corresponding XPL images of diagenetic phases in HEU-01-S1, 395.30 m. A, B) Dolomite generation post-dating C1 and pre-dating C2? Based on 1 thin section. C, D) Chemical compaction + calcite cemented veins, C3 – Equant calcite post-dating stylolites, pre-dating recrystallisation. E, F) Saddle dolomite occurrence. Dolomitizing fluid took advantage of thick stylolite. G, H) 502.70 m. One occurrence of fine crystalline dolomite along stylolite swarm.

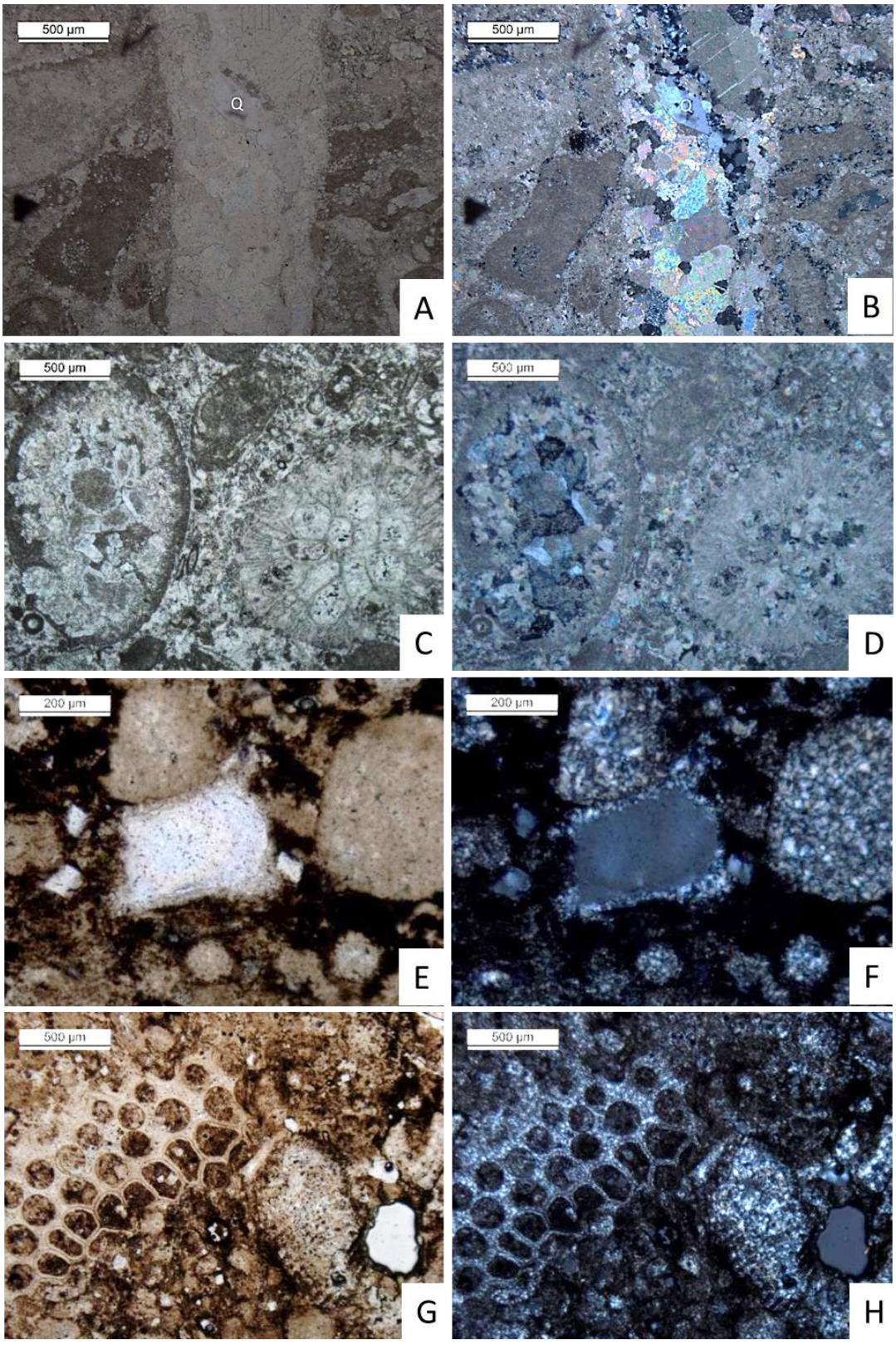

Figure 4-14: Photomicrographs showing the PPL and corresponding XPL images of silicification in HEU-01-S1. A, B) 483.25 m, silica post-dating C3. C, D) 119-120 m, silicification post-dates dolomitisation: dolomite rhombs are visible in the chert + rhombohedral pores occur in the chert. E, F) 224 m, silicification post-dates dolomitisation: dolomite rhombs are visible in the chert + rhombohedral pores occur in the chert. G, H) 224.60 m, the texture of the precursor limestone is preserved. It is possible that the precursor texture plays a role in the silicification process, i.e. all mudstones are silicified.

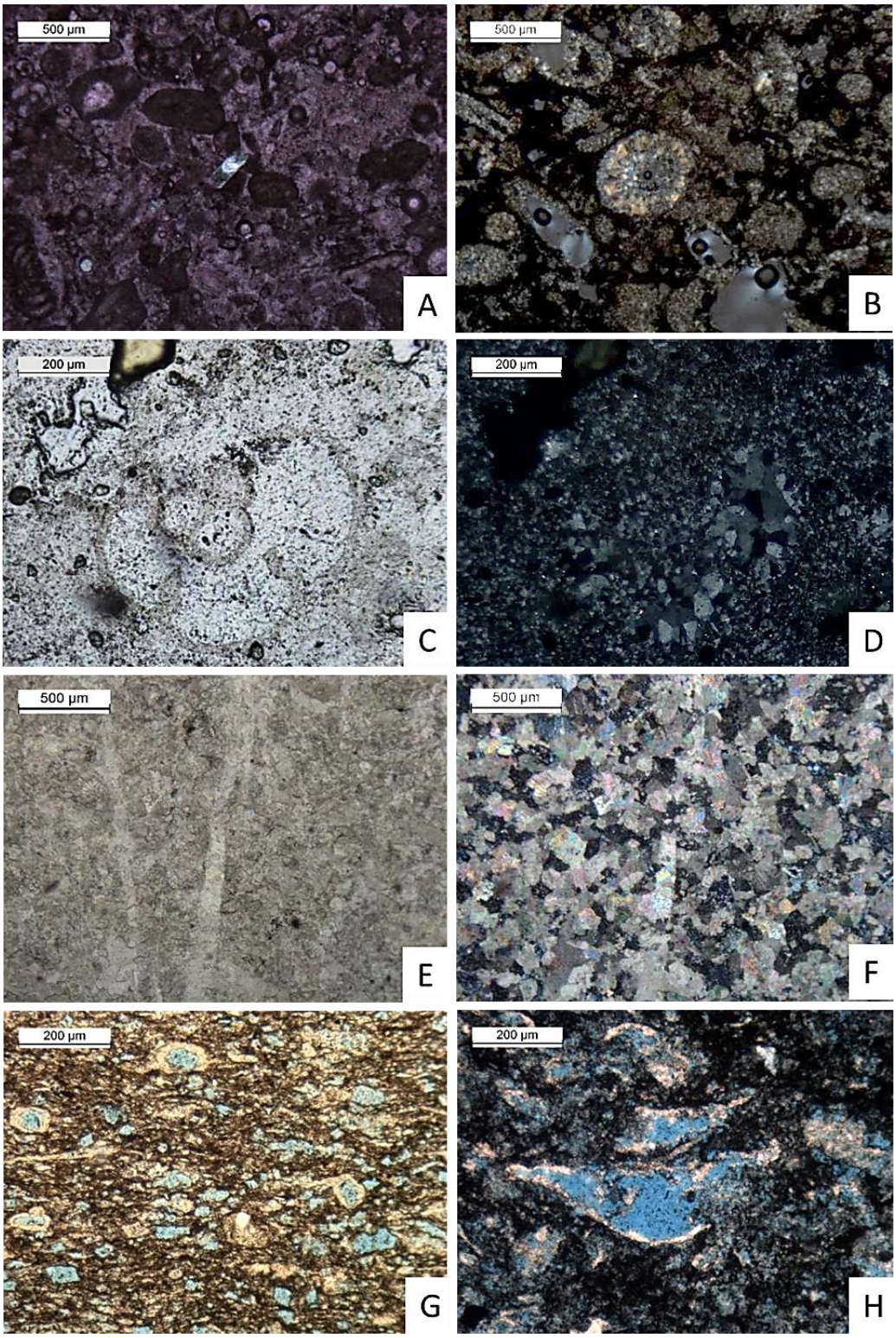

Figure 4-15: Photomicrographs showing the PPL and XPL images of diagenetic phases in HEU-01-S1. A) 360.2 m, partial silicification, lonely quartz crystal. B) Pervasive silicification, the texture of the precursor limestone is preserved. It is possible that the precursor texture plays a role in the silicification process, i.e. all mudstones are silicified. C, D) 225.10 m, pervasive silicification, the texture of the precursor limestone is preserved. It is possible that the precursor texture plays a role in the silicification process, i.e. all mudstones are silicified. E, F) 341.40 m, recrystallisation of bioclastic grainstone? by dolomite. G, H) 248.60 m, the silicification is associated with porosity (blue) in some rare cases. The porosity is either (secondary?) intraclast/shelter porosity or mouldic porosity after dolomite rhombs.

4.8 Additional data

Table 4-9: Vitrinite reflectance data for the HEU-01 well (Bless et al., 1981).

Depth (m)	Age	Rmax %	Samples	Remarks
220	V2a/V2b	5.26	7	Silty claystone with bituminous and pyritic schlieren. Small particles have been measured which are surely autochthonous, but cannot be identified with absolute certainty
227	V2a/V2b	5.36	10	Carbonaceous, pyritic claystone with some bituminous schlieren. Small poorly identifiable particles have been measured, which are certainly autochthonous.
261.5	V2a/V2b	5.06	12	Carbonate claystone with abundant inertinite
298.3-301.1	V2alV2b	5.04	5	Carbonate claystone with abundant bitumen. Bitumen frequently showing dissolution surface with mosaic structure.
316	V2a/V2b	5.25	12	Carbonate with abundant intergranular bitumen with reflectance between 3.57 and 4.5%.
333	V2a/V2b	5.17	9	Very clayey limestone. Only detrital particles in clayey streaks have been measured. One graphite particle with 8% Rmax.
349.5	V2a	5.06	2	Limestone with few usually inertinites organic particles
370.9	V2a	5.47	3	Limestone with reworked sapropelic clay. Vitrinite in reworked clay show Rmax of 6.77o (n: 8; s: 0.54).
384,9	V2a	5.88	7	Clayey limestone with abundant carbonaceous particles, most inertinites. Also, the measured particles show a slightly inert appearance.
401.7	V2a	6.27	25	Alternating laminae of clayey limestone and calcareous sapropelic claystone. No clear distinction between vitrinite and bitumen.
452.4	V2a	6.90	20	Calcareous, bituminous claystone with abundant vitrinite fragments. Rmax of bitumen between 4.8% and 6.2%.
469.2	V2a	6.76	5	Calcareous claystone to clayey limestone. Slightly sapropelic. With abundant carbonaceous particles, mostly bitumen. Graphites occur with 8.8% to more than 10% Rmax.
497.9	V2a	6.17 7.11	7 5	Clayey limestone with abundant inertinite. Certainly, autochthonous particles with distinct pleochroism have been measured. Differentiation into two groups of values may suggest different original substances (e.g. humic and bituminous). One graphite particle with 8.7% Rmax.

Table 4-10: Total and organic carbon content the HEU-01 well (Bless et al., 1981).

Depth (m)	Ctot%	Corg%
125.00-129.00	0.03	0.02
136.00-140.00	0.5	0.1
148.50-150.50	0.3	0.1
157.00-162.00	0.4	0.1
168.00-170.40	0.5	0.4
178.30-180.50	0.2	0.2
185.80-190.00	0.6	0.2
198.00-201.00	1.0	1.0
208.00-212.50	1.9	1.9
218.80-219.80	0.5	0.5
228.00-229.00	0.4	0.3
229.00		1.59
239.00-240.00	1	0.0
240.00		2.04
248.70	1.5	1.5
258.00-260.50	1.3	1.3
266.00		0.41
268.90-270.50	2.6	2.4
278.00-280.00	1.5	1.3
289.00-292.00	2	1.7
298.30-301.05	2.2	1.7
309.80	9.9	0.5
319.60	11.1	1.1
329.30		0.57
331.00	5.3	1.2
341.30	11.6	0.0
350.00		0.36
351.10	10.1	0.4
360.50	11.8	0.9
371.00	8.2	1.6
379.90	9.2	2.9
390.90	11.6	0.7
398.70	9.9	0.1
410.85	11.1	0.5
421.00	10.3	0.6
431.10	9.4	2.1
440.30	11.0	0.8
451.70	9.5	0.4
461.30	10.0	1.8
471.60	9.9	0.9
481.90	9.7	0.11
491.60	10.15	0.05
502.70	7.6	0.2

Table 4-11: Chemical analysis of major elemental concentrations from carbonates in HEU-01 and HEU-01-S1 (Bless et al., 1981).

Depth (m)	CaO %	MgO %	$CaCO_3$ %	$MgCO_3$ %
312.60-314.10	53.60	0.22	95.71r	0.46
320.00	52.71	2.01	93.16	4.22
341.60	32.39	18.12	57.84	38.05
356.80	51.82	0.41	92.54	0.86
364.50	53.74	0.45	95.96	0.95
365.40-365.60	53.79	0.45	95.98	0.94
385.85-386.05	44.96	0.58	80.22	1.21
391.35-391.50	45.56	0.60	81.29	1.26
401.25-401.50	22.68	0.47	40.47	0.98
408.05-408.30	44.47	2.71	79.35	4.41
439.80-440.00	50.75	1.00	90.55	2.09
458.75-459.00	51.85	0.94	95.52	1.97
501.70-502.00	46.44	0.66	82.86	1.38

Table 4-12: Chemical analysis in HEU-01 and HEU-01-S1 (Bless et al., 1981).

Depth (m)	LOI %	SiO2 %	TiO2 %	Al2O3 %	Fe2O3 %	MnO %	MgO %	CaO %
Heugem-01								
172	4.75	84.3	0.18	6.25	1.94	0.02	0.45	0.11
182.9	6.38	85.14	0.13	6.31	0.09	0	0.19	0.09
185.80-190.80	3.7	85.23	0.096	2.15	4.31	0.039	0.154	0.587
201.00-204.00	3.85	86.52	0.111	3.32	1.5	0.019	0.221	0.269
208.00-212.50	4.47	85.21	0.115	3.25	1.41	0.019	0.134	0.21
214	0.88	96.88	0.02	0.63	0.23	0	0.02	0.03
221	8.88	80.44	0.23	5.33	1.68	0.01	0.27	0.06
225.10-226.90	4.85	87.05	0.133	3.1	1.05	0.01	0.143	0.095
228	1.88	94.01	0.05	1.32	0.42	0	0.02	0.2
235.30-236.30	5.67	87.34	0.123	3.94	0.849	0.009	0.198	0.66
236	8.5	76.09	0.2	6.89	1.85	0.01	0.25	0.09
241.3	8.5	78.92	0.3	5.84	2.34	0.01	0.36	0.22
245.90-246.70	4.72	83.9	0.133	3.06	1.1	0.01	0.162	1.71
249.8	4.63	88.64	0.12	3.88	1.01	0.01	0.18	0.06
253.2	5.38	87.03	0.13	2.65	0.9	0.01	0.09	1.19
255 .70	2.1	93.07	0.07	1.52	0.62	0	0.06	0.46
262.4	2.63	93.45	0.06	1.6	0.66	0	0.03	0.11
264.6	1.63	94.87	0.03	0.82	0.31	0	0	0.85
271	4.88	85.43	0.08	2.21	0.85	0.01	1.29	2.25
280.00-283.00	4.84	81.88	0.105	2.65	3.21	0.029	0.295	2.03
286.00-289.00	6.24	81.45	0.122	3.4	2.01	0.019	0.778	2.58
298.30-301.00	5.54	82.74	0.094	2.32	2.05	0.019	0.623	2.38
306.00-309.00	3.34	90.05	0.087	2.19	0.706	0.01	0.155	0.135
330.30-332.20	16.47	60.33	0.025	0.551	0.125	0.033	0.192	21.99
333.10-335.30	15.06	63.31	0.034	0.713	0.153	0.034	0.212	19.35
338.6	38.63	9.59	0.02	0.36	0.19	0.01	0.11	49.08
339.6	10.38	74.02	0.01	0.41	0.2	0.03	0.04	12.86
Heugem-01-S1								
310.2	38.1	11.25	0.01	0.19	0.19	0.05	1.66	45.67
317.6	18.63	50.2	0.15	4.19	1.6	0.03	2.75	16.72
323.5	2.13	92.59	0.02	0.14	0.22	0	0.02	2.26
331.8	6.75	81.23	0.14	1.4	1.56	0.01	0.33	3.04
333.9	7.25	79.36	0.01	1.15	0.81	0.03	0.1	8.03
338.6	27	34.96	0.06	1.44	0.49	0.05	0.11	32.3
342.4	28.5	33.62	0.01	0.16	0.06	0.04	0.09	35.88
345.8	26	33.8	0.15	3.66	1.49	0.05	0.41	29.59
368.2	37.38	11.72	0.03	0.8	0.41	0.07	0.24	46.77
368.8	21.1	44.03	0.1	3.01	1.08	0.04	0.54	25.08
370.8	35	22.14	0	0.09	0.07	0.03	11.33	29.17
374.2	38.63	8.11	0.013	0.82	0.47	0.08	0.67	48.18
378.2	38.05	13.21	0.025	0.508	0.149	0.105	0.347	46.78
380.3	32.5	20.52	0.07	1.68	0.83	0.08	0.54	39.11
381.9	30.63	25.08	0.07	1.63	0.74	0.08	0.4	37.62
404	16.58	61.5	0.025	0.31	0.058	0.017	0.434	20.52

Table 4-13: Thin sections description in HEU-01 by Bless et al. (1981).

177.00 m	Cryptocrystalline to microcrystalline quartz, occasionally grading into quartz grains with a diameter of 0.08 mm. Isolated flakes of illite and sericite, and, aggregates of kaolinite. Irregularly distributed small sponge needIes(?) which appear as rounded to elliptical ghost structures. The presumed needles have been dissolved, leaving a cavity that in some cases is filled with kaolinite or rarely with cryptocrystalline quartz. Normally they have remained open. The outlines of the fossils are delineated by a narrow border of microcrystalline, irregular quartz grains (0.01 to 0.02 mm).
216. 90-217.10 m.	Silicified, carbonaceous calcilutite or calcisiltite with some ghosts of foraminifers. Presumably, the limestone has been dolomitised before silicification took place.
220,0 m.	Clayey-silty sapropel with abundant pyrite. Clay minerals almost completely obscured by organic substance. Only some sericite flakes can be recognised. Clastic quartz grains of silt size are regularly distributed or occur in clusters. Dark layers are enriched in organic matter and poor in silt. Extremely small pyrite grains (0.005 to 0.01 mm) occur.
227.2 m.	Clayey-silty sapropel with abundant pyrite and phosphate (crandallite). This slide resembles that from 220.0 m. But occasionally, the pyrite may reach a diameter of up to 0.025 mm.
229.00-229,60 m.	Silicified, carbonaceous peloid bioclastic packstone to grainstone. Grains very fine (0.04- 0.12 mm), well sorted. Some angular quartz grains of 30-90 µm.
231,4-232,0 m.	Porous mass of cryptocrystalline quartz with illite, sericite flakes, kaolinite (fireclay), coaly substance and very small pyrite grains. Isolated, angular to poorly rounded quartz grains (up to 0.1 mm Ø) occur. The coaly substance and pyrite occur in thin laminae and point to a primary deposit. Ghost structure of sponge needles(?) occur, like the ones described from 177.00 m.
235.30-236,50 m.	Silicified, carbonaceous bioclastic packstone.
236.50-237.50 m.	Silicified, carbonaceous bioclastic packstone. Relatively large pores.
251.30 253,50 m	Silicified, carbonaceous bioclastic calcarenite (packstone or grainstone). Bioclasts include foraminifers, algae and crinoids.
263,60 264.60 m	Silicified, carbonaceous clayey calcsiltite.
264,6 266,7 m	Porous rock with similar composition as sample 231.4-232.0 m. The principal difference consists in the occurrence of rhomb to cube-shaped pores of up to 0.05 mm Ø, which presumably represent ghosts of former dolomite crystals.
266.7 268,0 m	Groundmass of cryptocrystalline to microcrystalline quartz with finely disseminated carbonaceous material and pyrite, and optically invisible apatite. Abundant rhomb to cube-shaped pores and some dolomite crystals. Some radiolarians filled with microcrystalline quartz are visible.
268.9-270,5 m	Groundmass of cryptocrystalline to microcrystalline quartz and some kaolinite. Carbonaceous substance concentrated in a network-like pattern of schlieren, which enclose bright, graupen-like spots of microcrystalline quartz with some kaolinite (fireclay). Isolated light brown particles of collophane (cryptocrystalline apatite). Silicified or siliceous sponge needles occur.
349.40-349,70 m	Bioclastic packstone to grainstone. partly silicified. Remnants of foraminifers, crinoids and algae (Dasycladaceans). Grain size fine to medium.
360.72 m	Sparry calcite with carbonaceous, pyritic schlieren concentrated in network-like pattern enclosing spots of calcite. Quartz grains of silt size make up to 15% of the rock.

Table 4-14: Thin sections description in HEU-01-S1 by Bless et al. (1981).

361,60-361.70 m	Carbonaceous, partly silicified limestone. Isolated silicified or siliceous sponge needles.
366,95-367,00 m	Millimetric to micrometric alternation of micrite, biomicrite, biosparite, intrasparite. Parallel laminations. Micrometric laminae of organic substance (algal layers2). Numerous Umbellinae.
365.80-368.90 m	Biomicritic grading into biosparite with local lenses of anhydrite.
369.70 369.85 m	Carbonaceous, sparitic limestone. Carbonaceous material partly concentrated in schlieren, partly finely disseminated.
383.40 383.60 m	Biomicrite grading into biointrasparite with micrometric intercalations of laminae consisting of organic substance (algal layers?). Rare angular detrital quartz grains are dispersed in the calcite matrix. Important intergranular porosity.
390.20 m	Biomicrite with joints which are either oblique or parallel to the stratification. These joints are filled with calcite which may show geopetal features or be fibrous or even saccharoidal (calcite pseudomorphs after anhydrite, associated with anhydrite). The horizontal joints are separated from the micrite by very fine laminae of black organic material (algal layers?).
397 m	Biomicrite with conglomeratic to breccia intercalations. Abundance of caicispheres and foraminifers. Very fine laminae of organic substance (algal layers?). Breccias consist of angular fragments of metamorphic quartzite (quartz with undulated extinction and breached contacts between the grains), micaceous pelite, pelitic material that resembles an altered volcanic ash, and anhydrite fragments. Anhydrite also occurs as partial filling of a bryozoan.
407.75 m	Alternation of fine laminae consisting of saccharoidal dolomite, biomicrite with abundant organic material (algal debris), biomicrite with network like pattern of organic material, micrite grading into microsparite, bio micrite with abundant calcispheres, slightly micaceous dolomitised biosparite, and laminae consisting of organic material (algal layers?).
477 m	Biomicrite with finely disseminated organic substance; slightly quartziferous. Bioclasts show graded bedding. Important intergranular porosity.
454.90 m	Finely laminated biomicrite with numerous' sometimes anastomosing small joins filled with sparry calcite. Few quartz grains. 501.90 m, Biomicrite with network of joints filled with sparry calcite. Very few angular quartz grains.

This page intentionally left blank

Daalsesingel 1
3511 SV Utrecht
scan@ebn.nl
www.scanaardwarmte.nl

Onderzoek in de ondergrond voor aardwarmte